

## Origin of Magnetic and Magnetoelastic Tweedlike Precursor Modulations in Ferroic Materials

A. Saxena,<sup>1,2</sup> T. Castán,<sup>1</sup> A. Planes,<sup>1</sup> M. Porta,<sup>1</sup> Y. Kishi,<sup>3</sup> T. A. Lograsso,<sup>4</sup> D. Viehland,<sup>5</sup> M. Wuttig,<sup>3</sup> and M. De Graef<sup>6</sup>

<sup>1</sup>*Department d'Estructura i Constituents de la Matèria, Universitat de Barcelona, Diagonal 647, 08028 Barcelona, Spain*

<sup>2</sup>*Theoretical Division, Los Alamos National Laboratory, Los Alamos, New Mexico 87545, USA*

<sup>3</sup>*Department of Materials Science and Engineering, University of Maryland, College Park, Maryland 20742, USA*

<sup>4</sup>*Ames Laboratory, Iowa State University, Ames, Iowa 50011, USA*

<sup>5</sup>*Department of Materials Science and Engineering, Virginia Tech, Blacksburg, Virginia 24060, USA*

<sup>6</sup>*Department of Materials Science and Engineering, Carnegie Mellon University, Pittsburgh, Pennsylvania 15213, USA*

(Received 16 September 2003; published 14 May 2004)

Based on experimental observations of modulated magnetic patterns in a  $\text{Co}_{0.5}\text{Ni}_{0.205}\text{Ga}_{0.295}$  alloy, we propose a model to describe a (purely) magnetic tweed and a magnetoelastic tweed. The former arises above the Curie (or Néel) temperature due to magnetic disorder. The latter results from compositional fluctuations coupling to strain and then to magnetism through the magnetoelastic interaction above the structural transition temperature. We discuss the origin of purely magnetic and magnetoelastic precursor modulations and their experimental thermodynamic signatures.

DOI: 10.1103/PhysRevLett.92.197203

PACS numbers: 75.80.+q, 62.20.Dc, 64.70.Kb, 75.30.Kz

The thermodynamics of phase transitions is strongly influenced by the presence of quenched disorder [1]. In particular, statistical compositional disorder plays a fundamental role in the precursor strain modulations observed in alloys undergoing a first-order displacive transition [2]. Such strain modulations are crosshatched and give rise to the so-called (structural) tweed pattern [3] observed well above the transition temperature  $T_M$  [4]. Recent advances in high resolution imaging of magnetic domain patterns, such as magnetic force microscopy [5] and Lorentz transmission electron microscopy (LTEM) [6], have revealed fascinating modulated magnetic patterns both above and below the Curie temperature in certain magnetic alloys. In contrast to the structural tweed, the magnetic modulations that occur as precursors to the magnetic transition give rise to a stripelike pattern.

In this Letter we present TEM observations in  $\text{Co}_2\text{NiGa}$  alloys showing both strain and magnetic modulations and provide a model that explains these observations. We focus on the magnetic modulations and demonstrate that the tweed concept is not just structural but applicable to a much broader class of materials. We show that, independently of specific details of the pattern or the physical variable involved in modulation, the origin of tweed lies in very general requirements in quite different materials undergoing phase transitions. For instance, polar (or dielectric) tweed has been observed in mixed  $B$ -site cation ferroelectrics, such as  $\text{Pb}(\text{Mg}_{1/3}\text{Nb}_{2/3})_3\text{-PbTiO}_3$  [7]. Extending previous ideas in the context of (purely) structural tweed [2], we suggest that the tweedlike modulations above the transition (structural, magnetic, or other) are a natural cooperative response in systems that are sensitive (in the sense of, e.g., phonon softening, “susceptibility” or other response functions) to local symmetry breaking perturbations (e.g., due to statistical disorder) assisted by anisotropic long-range interactions. The long-range nature of such

interactions (elastic, magnetic, or other) connects the different perturbed regions while the anisotropy determines the specific modulations of the resulting pattern. We note that statistical compositional disorder is intrinsic to alloys and therefore they are the most probable candidates to exhibit such phenomena.

We start by defining what we mean by magnetic tweedlike patterns. Analogous to structural tweed, magnetic tweed is diffraction contrast present in TEM observations, corresponding to modulations in the magnetization (instead of strain) above the Curie temperature  $T_c$  (instead of the structural transition temperature  $T_M$ ). There are three common ingredients necessary to stabilize tweed patterns, regardless of structural, magnetic, or other physical variables: (i) The material system must be “sensitive” to local symmetry breaking perturbations. That is, there is a softening of the relevant elastic constants or phonons (inverse magnetic susceptibility or magnons) with temperature. This soft lattice behavior (“spin stiffness”) sensitively responds to local disorder. Consequently, there is a local variation of the structural (magnetic) transition temperature giving rise to local transformed regions above the nominal  $T_M$  ( $T_c$ ). (ii) There must be long-range interactions caused by elastic compatibility constraints (magnetic dipole forces arising from the surface of the crystal). Such interactions enable connections between the local transformed regions mentioned above, thereby stabilizing them. (iii) To obtain a specific modulation pattern, one needs anisotropy to select modulations along specific directions. For the structural tweed, this is contained in the long-range elastic interactions due to the crystal symmetry and elastic compatibility [8]. In the magnetic case, long-range anisotropy (including shape anisotropy) is well accounted for by the dipolar interaction [9].

The magnetic tweedlike modulations could conceivably arise in two different ways: (i) purely due to

magnetic disorder without any structural degrees of freedom being involved. This can be called purely magnetic tweed or simply magnetic tweed. It has been (likely) observed above the Curie temperature ( $T_c$ ) in  $\text{Co}_{0.38}\text{Ni}_{0.33}\text{Al}_{0.29}$  alloys [10]. (ii) Because of structural or compositional disorder which produces a structural tweed above the structural transition temperature ( $T_M$ ) in magnetic alloys undergoing a martensitic transition. A coupling of strain with magnetism can then lead to a magnetic modulation both above and/or below  $T_c$ . We label this kind of tweed magnetoelastic tweed. As described in the following paragraphs, it has been observed by LTEM in ferromagnetic (Heusler)  $\text{Ni}_2\text{MnGa}$  [11,12] and  $\text{Co}_2\text{NiGa}$  alloys. By using two-dimensional models on a square lattice we will show that magnetic tweed patterns are stripelike whereas magnetoelastic tweed produces crosshatched patterns. Crystals of Co-Ni-Ga were grown by the Bridgman method. Thin sections were prepared for TEM and selected area electron diffraction studied by standard specimen preparation methods. The TEM studies were carried out on a JEOL 4000EX atomic resolution microscope operating at 400 kV, and a Philips CM20, operated at 200 kV. The 400 kV system is equipped with a Gatan imaging filter which compensates for the magnification loss due to the increased focal length of the Lorentz imaging mode and also permits removal of inelastically scattered electrons to enhance the image contrast. Imaging of ferroelastic or structural domains was performed using the conventional bright-field mode, whereas imaging of the ferromagnetic domain structure was performed using Lorentz microscopy.

TEM observations were carried out on a  $\text{Co}_{0.5}\text{Ni}_{0.205}\text{Ga}_{0.295}$  alloy that was quenched from 1200 K. This alloy was chosen so that both structural transformation,  $T_M$ , and Curie temperatures,  $T_c$ , were located below and above room temperature, respectively, i.e.,  $T_M \approx 148$  K and  $T_c \approx 393$  K, as determined by elastic spectroscopy and vibrating sample magnetometry. All TEM observations were obtained in the ferromagnetic austenite phase. Figure 1 shows a bright-field image of the (400) bend contour of Co-Ni-Ga, taken at room temperature near the [110] zone axis orientation. The image reveals ferroelastic or structural domains. Tweedlike contrast can be seen, with a characteristic length scale of about 10 nm. In this image, the crosshatched tweed patterns are clearly evident on both sides of the bend contour. In electron diffraction patterns, diffuse streaks along the  $\langle 110 \rangle$ -type directions were observed, typical for tweed modulated structures. Figure 2 shows a through-focus series of Fresnel Lorentz images for Co-Ni-Ga. Figure 2(c) is the in-focus image and it shows tweed contrast near the central bend contour. The underfocus 2(a) and overfocus 2(b) images show strong striations of a length scale similar to that of the tweed striations. Since these striations are visible only in the out-of-focus images, they must be ascribed to magnetic modulations. This is further shown in Fig. 2(d), which is the difference between

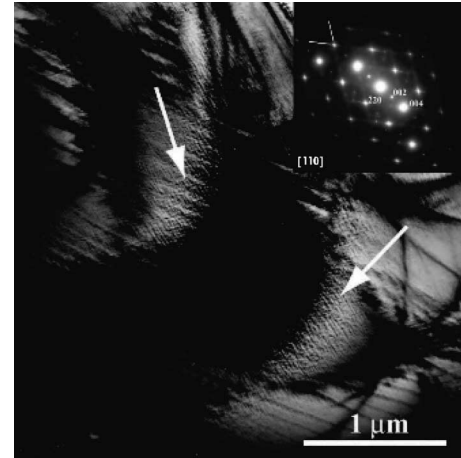


FIG. 1. Bright field image and corresponding electron diffraction pattern (inset) for the near [110] zone axis orientation of  $\text{Co}_{0.5}\text{Ni}_{0.205}\text{Ga}_{0.295}$ . The tweed contrast (arrows) near the (004) bend contour is consistent with the diffuse streaks along apparent [112] directions (solid white lines in the diffraction pattern). B2 superlattice reflections are clearly present.

images (a) and (b). This difference image is proportional to the Laplacian of the magnetic component of the phase of the electron wave [13], which indicates a magnetic origin for the striations. The coincident elastic and magnetic modulations have a wavelength in the range of 50–100 nm. Tweedlike striations identical to those shown in Figs. 1 and 2 have been observed previously by TEM at temperatures above the transformation temperature,  $T_M$ . Upon cooling below  $T_M$ , those striations condense into micron size twin structures through an adaptive metastable phase. The structural tweed contrast in paramagnetic austenites is elastically driven.

We anticipate that magnetoelastically driven magnetic tweed will equally condense into ferromagnetic

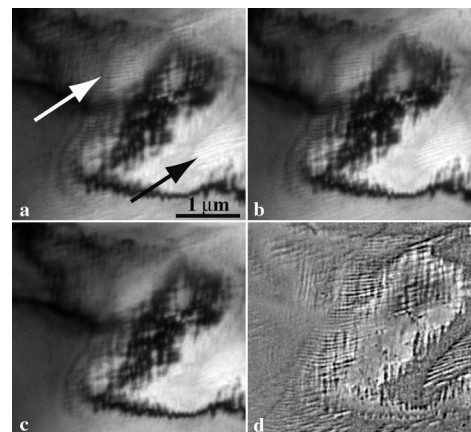


FIG. 2. Zero-loss underfocus (a) and overfocus (b) images (Fresnel imaging mode, 400 kV) of a region near a bend contour. The in-focus image (c) shows tweed contrast, and the out-of-focus images reveal the presence of an additional modulated structure (arrowed) which is magnetic in nature. (d) shows the difference between (a) and (b). Contrast variations in (d) are indicative of magnetic tweed.

martensite. The dual, magnetic and elastic, nature of the tweed demonstrated in Fig. 2 must be the result of magnetoelastic coupling. In ferromagnets like Fe or Ni, the magnetoelastic energy of a domain wall is only a fraction of its total energy. This is no longer true in elastically soft ferromagnetic materials. For instance, in materials for which the elastic constants obey the relations  $(C_{11} - C_{12}) \ll C_{44}$ ,  $(C_{11} + 2C_{12})$ , and the magneto-crystalline energy is positive, the magnetoelastic coupling causes the energy of  $\langle 100 \rangle$   $180^\circ$  domain walls,  $E_{100}$ , to be larger than that of  $\langle 110 \rangle$   $90^\circ$  walls,  $E_{100} > E_{110}$ . Since the elastic condition is met in several mar-

tenisitic transformations, and there are indications of shear elastic softness in Co-Ni-Ga, we propose that the observed coincident elastic and magnetic tweed is, in fact, magnetoelastic tweed of the kind that will naturally condense into  $\langle 110 \rangle$   $90^\circ$  walls upon transformation. Thus the magnetic tweed is a unique type of domain organization that results from the multiferroic characteristics of the material. A definitive experimental observation supporting magnetoelastic coupling is the change in elastic constants with the application of a magnetic field [14].

Let us consider the following Ginzburg-Landau model to describe the magnetoelastic tweed:

$$F(\phi, m, \eta) = [A(T - T_0) + A_\eta(\eta - \eta_0) + A_m(m^2 - m_0^2)]\phi^2 + b\phi^4 + c\phi^6 + K_1(\nabla\phi)^2 + K_2(\partial_x^2\eta - \partial_y^2\eta)\phi + K_3(m_x^2 - m_y^2)\phi + K_4(\partial_x^2m - \partial_y^2m)\phi + K_5m^2\phi^2 + \alpha m^2 + \beta m^4 + \mu \int dxdy \frac{\phi(r)\phi(r')}{|r - r'|^2},$$

where  $\phi$  is the deviatoric (rectangular) strain driving the structural transition starting from a square lattice,  $\eta$  denotes the statistical (compositional or structural) disorder and  $\mathbf{m} = (m_x, m_y)$  is the magnetization [15]. Note that the structural transition is locally modified by both the structural and magnetic disorder (as usual, both are assumed to have a spatial Gaussian distribution around mean values  $\eta_0$  and  $m_0$ , respectively).

The model includes two alternative strain-disorder couplings: (i) statistical disorder (around mean values) either structural  $(\eta - \eta_0)$  or magnetic  $(m^2 - m_0^2)$  and (ii) substitutional disorder associated with the term  $(\partial_x^2\eta - \partial_y^2\eta)$ . This last term is due to local gradients in the alloy concentration (i.e., a local conservation) and has been studied previously [2]. Local gradients in the magnetization coupling to strain are also considered. Other forms of disorder such as impurities or vacancies which are not essential to produce tweed are not considered here. We focus on those quenched disorders which change locally the transition temperature. Note that even though there is no magnetic disorder, structural (or compositional) disorder is sufficient to cause local (static) variations in the effective free-energy to result in magnetoelastic tweed contrast. The key ingredient is the anisotropic long-range interaction (of strength  $\mu$ ) originated from the geometrical constraints of the lattice [8]. For a square lattice strain modulations occur indeed along the diagonals [2,8].

To describe magnetic tweed the only relevant degrees of freedom are magnetic. Assuming as before a Gaussian spatial distribution of magnetic disorder denoted by  $\eta$  (around a mean  $\eta_0$ ), we have [15]

$$F(m, \eta) = [A(T - T_c) + A_\eta(\eta - \eta_0)]m^2 + \beta m^4 + Km_x^2m_y^2 + \frac{\gamma}{2}(\nabla m)^2 + (\partial_x^2\eta - \partial_y^2\eta)m^2 + g \int dxdy \left[ \frac{\mathbf{m} \cdot \mathbf{m}'}{r^2} - 2 \frac{(\mathbf{m} \cdot \mathbf{r})(\mathbf{m}' \cdot \mathbf{r})}{r^4} \right].$$

We have included the long-range dipolar interaction,

often ignored in theoretical models but always present in real magnetic systems. Again, the statistical disorder locally modulates the transition temperature. The  $K > 0$  term breaks the continuous degeneracy on the  $xy$  plane and selects the  $x$  or the  $y$  direction.  $\gamma$  is a measure of the creation energy of a magnetic domain wall,  $A$  is the inverse magnetic susceptibility which has the right softening behavior with temperature, and  $g$  is the strength of the magnetic dipolar interaction between two dipoles connected by  $\mathbf{r}$ . All terms considered in conjunction with the short-range gradient term and the long-range dipolar interaction thus stabilize the magnetic tweed in a certain regime of the parameter space. It is easy to see that the magnetic dipole interaction in 2D can be expressed, with  $k^2 = k_x^2 + k_y^2$ , as [16]

$$F_d^m = g \int \frac{dk}{k^2} \{ (k_x^2 - k_y^2) [m_x(k)m_x(-k) - m_y(k)m_y(-k)] + 2k_xk_y [m_x(k)m_y(-k) + m_y(k)m_x(-k)] \}.$$

Note that  $k_x^2 - k_y^2 = k^2 \cos 2\phi$  and  $2k_xk_y = k^2 \sin 2\phi$  which indicates that the anisotropy [9] of this long-range interaction does not correspond to the crosshatched tweed pattern seen in structural transitions but rather to a horizontal or a vertical modulation (corresponding to the  $2\phi$  term). Stripelike magnetic domains have been indeed observed above the Curie point in Co-Ni-Al using Lorentz microscopy [10].

To emphasize the analogy between both models, we show that the elastic compatibility condition is formally equivalent to an elastic dipole interaction.

Consider the following free-energy for a square lattice:  $F = (A_1/2)e_1^2 + (A_2/2)e_2^2 + (A_3/2)e_3^2 + f_{nl}(e_2, e_3)$ , where the symmetry-adapted strains given by the dilatation  $e_1$ , deviatoric strain  $e_2$ , and shear  $e_3$  have the usual definition in terms of the Lagrangian strain tensor [17].  $A_1$ ,  $A_2$ , and  $A_3$  denote, respectively, the bulk, deviatoric, and shear moduli. For structural phase transitions involving either  $e_2$  or  $e_3$ , the nonlinear term  $f_{nl}(e_2, e_3) \neq 0$ , but for simple

elastic deformation it is zero. In either case, since the  $e_1$  term does not break the symmetry, we can express it in terms of  $e_2$  and  $e_3$  by using the elastic compatibility condition in 2D (for geometrically linear strains) [8]. We obtain (in  $k$  space)

$$F_d^e = \frac{A_1}{2} e_1^2 = \frac{A_1}{2} \int \frac{dk}{k^4} \{ (k_x^2 - k_y^2)^2 e_2^*(-k) e_2(k) + (2k_x k_y)^2 e_3^*(-k) e_3(k) + 2k_x k_y (k_x^2 - k_y^2) [e_2^*(-k) e_3(k) + e_3^*(-k) e_2(k)] \}.$$

We now define an “elastic dipole vector”  $\mathbf{D}(q) = (D_x(q), D_y(q)) = (1/\sqrt{2})(e_2, e_3)$  and the generalized [18] “wave vector”  $\mathbf{q} = (q_x, q_y) = (2k_x k_y, k_x^2 - k_y^2)$ . Then the above equation can be expressed, with  $q^2 = q_x^2 + q_y^2 = k^4$ , as

$$F_d^e = \frac{A_1}{2} \int \frac{dq}{q^2} \{ q^2 [\mathbf{D}^*(-q) \cdot \mathbf{D}(q)] - 2[\mathbf{D}^*(-q) \cdot \mathbf{q}][\mathbf{D}(q) \cdot \mathbf{q}] \}.$$

This is the elastic dipole interaction [19] energy which has formally the same structure as the 2D magnetic (or polar) dipole interaction energy given above [16]. However, a close scrutiny of the  $k$ -space expression reveals that the anisotropy of the long-range interaction is different. Note that  $(k_x^2 - k_y^2)^2 = \cos^2 2\phi$ ,  $(2k_x k_y)^2 = \sin^2 2\phi$ , and  $2k_x k_y (k_x^2 - k_y^2) = (1/2) \sin 4\phi$ . Again, we obtain that the anisotropy of this long-range elastic interaction corresponds to a crosshatched (tweed) pattern due to  $\sim \sin 4\phi$  and  $\sim \cos 4\phi$  leading terms.

The concept of a structural or a magnetic tweed can be generalized to a “ferroelastic tweed.” A “proper” ferroelastic tweed would correspond to strictly the structural tweed [2,8]. However, magnetic tweed (in magnetic or magnetoelastic materials) and polar tweed in ferroelectrics [20] would correspond to “improper” ferroelastic tweed because both the disorder and the long-range interaction may arise from a physical variable other than strain, e.g., magnetization or polarization. Improper ferroelastic tweed may also be observable in Jahn-Teller distorted colossal magnetoresistance (CMR) materials, charge-density-wave high  $T_c$  superconductors, and other perovskites with disorder in, for instance, octahedral tilts. The long-range interaction in improper ferroelastic tweed is due to magnetic dipolar or electric dipolar interaction with a different kind of anisotropy than in the structural case. Thus, one would expect different tweed patterns for the proper and improper ferroelastic tweed. The softening in magnetic tweed may correspond to magnon modes. Similarly, in ferroelectric tweed it may be associated with “polar” (or optical) phonons.

In summary, we have observed modulated magnetic patterns in a  $\text{Co}_2\text{NiGa}$  alloy and presented a model for both the magnetic and magnetoelastic tweed and contrasted these with a structural tweed. The type of anisotropy and the long-range interaction are crucial in determining the nature of the resulting pattern. The giant magnetoresistance materials [21], superconductors [22], and CMR materials can also exhibit such tweedlike modulations. Indeed, these materials seem to possess the three common ingredients required for tweed formation.

A.S. acknowledges support from Iberdrola (Spain). This work was supported by the U.S. Department of Energy (DOE), the CICyT (Spain) Project No. MAT2001-

3251 and CIRIT (Catalonia) Project No. 2001SGR00066, the U.S. National Science Foundation, Grants No. DMR0095166 and No. DMR-0095586, the Office of Naval Research, Contracts No. MURI N000140110761, No. N000149910837, and No. N000140010849, as well as the DOE No. DE-FG02-01ER45893. M. D. G. acknowledges the Research Council of the University of Antwerp (Belgium) for partial financial support during a sabbatical research visit at the EMAT laboratory. T. A. L. acknowledges the support of the Office of Basic Energy Sciences, Materials Sciences Division, of the U.S. DOE under Contract No. W-7405-ENG-82.

- [1] Y. Imry and M. Wortis, *Phys. Rev. B* **19**, 3580 (1979).
- [2] S. Kartha *et al.*, *Phys. Rev. Lett.* **67**, 3630 (1991); *Phys. Rev. B* **52**, 803 (1995), and references therein.
- [3] The origin of the term tweed [L. E. Tanner, *Philos. Mag.* **14**, 111 (1966)] comes from the striations observed in bright-field TEM.
- [4] S. M. Shapiro *et al.*, *Phys. Rev. Lett.* **57**, 3199 (1986).
- [5] R. D. Gomez, in *Experimental Methods in the Physical Sciences*, edited by M. De Graef and Y. Zhu (Academic, San Diego, 2001), Vol. 36, p. 69.
- [6] M. De Graef, in *Experimental Methods in the Physical Sciences* (Ref. [5]), p. 27.
- [7] Z. Xu *et al.*, *Philos. Mag. A* **74**, 395 (1996).
- [8] S. R. Shenoy *et al.*, *Phys. Rev. B* **60**, R12537 (1999).
- [9] Short-range anisotropy such as magnetocrystalline and magnetostriction, although relevant in other contexts, is not essential here. See, e.g., G. Bertotti, *Hysteresis in Magnetism* (Academic, San Diego, 1998).
- [10] Y. Murakami *et al.*, *Acta Mater.* **50**, 2173 (2002).
- [11] Y. Kishi *et al.*, *J. Phys. IV (France)* **112**, 1021 (2003).
- [12] H. S. Park *et al.*, *Appl. Phys. Lett.* **83**, 3752 (2003).
- [13] M. De Graef, *Introduction to Conventional Transmission Electron Microscopy* (Cambridge University Press, Cambridge, 2003), Chap. 10.
- [14] A. Planes *et al.*, *Phys. Rev. Lett.* **79**, 3926 (1997).
- [15] A. N. Vasil'ev *et al.*, *Phys. Rev. B* **59**, 1113 (1999).
- [16] B. P. Stojković *et al.*, *Phys. Rev. B* **62**, 4353 (2000).
- [17] G. R. Barsch and J. A. Krumhansl, *Phys. Rev. Lett.* **53**, 1069 (1984).
- [18] For the dyadic notation, see, e.g., K. R. Symon, *Mechanics* (Addison Wesley, Reading, MA, 1971).
- [19] The form remains unchanged if we choose to eliminate  $e_2$  (or  $e_3$ ) provided we redefine the dipole vector.
- [20] O. Tikhomirov *et al.*, *Phys. Rev. Lett.* **89**, 147601 (2002).
- [21] L. Yiping *et al.*, *Phys. Rev. B* **54**, 3033 (1996).
- [22] S. Sergeenkov and M. Ausloos, *Phys. Rev. B* **52**, 3614 (1995).